

Dependence of enhanced Kerr nonlinearity on coupling power in a three-level atomic system

Hai Wang,* David Goorskey, and Min Xiao

Department of Physics, University of Arkansas, Fayetteville, Arkansas 72701

Received September 7, 2001

We study the enhanced Kerr-nonlinear coefficient in a three-level Λ -type atomic system for various coupling-beam powers. The Kerr-nonlinear coefficient behaves very differently in the strong and the weak coupling power regions and changes sign when the coupling or probe frequency detuning changes sign. Comparisons of Kerr-nonlinear coefficients as functions of probe frequency detuning, coupling power, and coupling frequency detuning are presented. © 2002 Optical Society of America

OCIS codes: 190.3270, 030.1670, 160.4330, 120.5050.

Nonlinear optical processes can be greatly enhanced by atomic coherence in three-level atomic systems. In the past few years several experimental demonstrations of enhanced nonlinear optical processes in multilevel atomic systems were reported.¹⁻⁵ These experiments prompted recent theoretical studies of nonlinear optics at the single-photon level in three-level or four-level atoms.⁶⁻⁸ More recently, the enhanced Kerr-nonlinear coefficient (n_2) of a three-level atomic system was directly measured by use of an optical ring cavity under conditions of electromagnetically induced transparency (EIT); i.e., the coupling intensity is much larger than the probe intensity.⁹ These measurements provide a good understanding of the enhanced Kerr nonlinearity near EIT resonance and the possibility of optimizing nonlinear optical processes. However, enhancing the nonlinear optical processes is a property that is not unique to conditions of EIT alone. It also occurs near more-general coherent population trapping conditions for an arbitrary ratio of coupling power to probe power in three-level atomic systems.

In this Letter we present our experimental measurements of enhanced n_2 under general conditions of coherent population trapping when the coupling beam's power is varied from nearly equal to the probe power to much larger than the probe power. At the exact condition of coherent population trapping, i.e., when both the coupling frequency and the probe frequency detunings are zero, n_2 is zero. However, when one of the frequency detunings is tuned slightly off resonance, n_2 can be enhanced as much as 2 orders of magnitude compared with the value of n_2 when there is no coupling beam and can also change sign depending on the frequency detunings of the coupling and the probe beams. n_2 behaves quite differently in the strong- and the weak-coupling-beam limits.

Our experimental setup is the same as the one used for measuring n_2 under EIT conditions.⁹ A rubidium vapor cell (5 cm in length and heated to 67 °C) with Brewster windows wrapped in a magnetic-shielding metal sheet is placed in an optical ring cavity (with a three-mirror configuration) with a length of 37 cm. The probe beam enters the ring cavity through one mirror (concave, with $R = 10$ cm and a transmissivity of 3%) and circulates inside the cavity.

It exits the cavity through an output coupler with 1% transmission. The coupling beam is introduced through a polarization beam splitter cube inside the optical cavity with an orthogonal polarization to the probe beam. The coupling beam is misaligned from the probe beam at an angle of $\sim 2^\circ$, so it does not circulate inside the ring cavity. The radii of the coupling and the probe beams at the center of the atomic cell are estimated to be 700 and 80 μm , respectively. The empty-cavity finesse is ~ 100 but degrades to ~ 50 after insertion of the atomic cell (with atoms far from resonance) and the polarization beam splitter cube.

We consider the three-level Λ -type atomic system in ^{87}Rb $D1$ lines. The coupling beam with frequency ω_c is coupled to near the $5S_{1/2}, F' = 2 - 5P_{1/2}, F' = 2$ transition of frequency ω_{23} , and the probe beam with frequency ω_p is tuned near the transition from $5S_{1/2}, F = 1$ to $5P_{1/2}, F' = 2$ (frequency, ω_{12}). The coupling and probe frequency detunings are defined as $\Delta_p = \omega_p - \omega_{21}$ and $\Delta_c = \omega_c - \omega_{23}$, respectively, and their values are set by use of saturation absorption spectroscopy. The essential scheme that saves us from experiencing large Doppler broadening at such temperatures in an atomic cell is the use of a two-photon Doppler-free configuration^{10,11} setup by propagation of the coupling and probe beams in the same direction. The technique of using an optical cavity to measure a Kerr-nonlinear coefficient has advantages over other (such as Z-scan) methods for atomic systems, because it can work with low laser intensity and long atomic cells. The well-defined cavity mode also prevents spatial changes in the probe beam owing to the nonlinearity in our experiment.

With ω_c and ω_p locked to certain values, we scan the length of the optical ring cavity across resonance by applying a ramp voltage to a piezoelectric transducer mounted upon the third cavity mirror (high reflector). When the coupling beam is blocked, the cavity transmission profile is basically symmetric, as shown in Fig. 1(a), with $\Delta_p = +40$ MHz and an intracavity peak power of 6 μW (corresponding to an intracavity peak Rabi frequency of $\Omega_p = 2\pi \times 11$ MHz). When the coupling beam is turned on with a power of 1.1 mW (corresponding to an average Rabi frequency of $\Omega_c = 2\pi \times 17$ MHz inside atomic cell) and $\Delta_c = 0$,

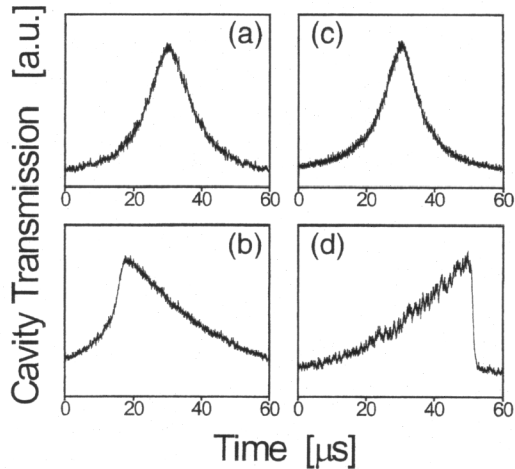


Fig. 1. Cavity transmission profiles for (a) $\Delta_p = 40$ MHz and $\Omega_c = 0$; (b) $\Delta_p = 40$ MHz and $\Omega_c = 2\pi \times 17$ MHz; (c) $\Delta_p = 7$ MHz and $\Omega_c = 0$; (d) $\Delta_p = 7$ MHz and $\Omega_c = 2\pi \times 72$ MHz. $\Delta_c = 0$.

the cavity transmission profile becomes asymmetric, as shown in Fig. 1(b). This asymmetry in the cavity transmission profile is caused by the Kerr-nonlinearity-induced phase shift in the three-level atomic system enhanced by atomic coherence. Kerr-nonlinearity-induced phase shift in the three-level atomic system enhanced by atomic coherence. Kerr-nonlinearity-induced phase shift in the three-level atomic system enhanced by atomic coherence. Kerr-nonlinearity-induced phase shift in the three-level atomic system enhanced by atomic coherence. Kerr-nonlinearity-induced phase shift in the three-level atomic system enhanced by atomic coherence. Kerr-nonlinearity-induced phase shift in the three-level atomic system enhanced by atomic coherence.

When the coupling power is increased, n_2 behaves differently. For the coupling power of $P_c = 20$ mW (corresponding to $\Omega_c = 2\pi \times 72$ MHz inside the atomic cell), $\Delta_c = 0$, $\Delta_p = +7$ MHz, and $\Omega_p = 2\pi \times 11$ MHz, the cavity transmission profile is also asymmetric, as shown in Fig. 1(d). The asymmetrical profiles in Figs. 1(b) and 1(d) are opposite each other, which indicates that the signs of n_2 are also opposite, even though the frequency detunings have the same sign. Figure 2(b) plots n_2 as a function of Δ_p for $\Delta_c = 0$, $\Omega_p = 2\pi \times 11$ MHz, and $\Omega_c = 2\pi \times 72$ MHz. Although the maximal values of n_2 are similar in weak- and strong-coupling beams, their dependence on frequency detuning is quite different. The main features of measured n_2 as a function of Δ_p near resonance include the growth of the center peaks from as small as in Fig. 2(a) to very large as in Fig. 2(b) and the movement of the large peaks in Fig. 2(a) to higher probe frequency detunings as in Fig. 2(b). The differences in n_2 values between three-level (filled squares) and the two-level (open circles) cases at high frequency detunings (beyond ± 200 MHz) in Fig. 2(b) are due to optical pumping with the strong coupling beam.

To study the change of n_2 as a function of P_c , we chose one probe frequency detuning for each of the weak and strong coupling powers. Because the

maximal value of n_2 was measured at $\sim \Delta_p = 40$ MHz with $P_c = 1.1$ mW, we measured n_2 as a function of P_c by keeping $\Delta_c = 0$ and $\Omega_p = 2\pi \times 11$ MHz. The measured data are plotted in Fig. 3(a). The Kerr nonlinearity increases quickly as the coupling power increases, and it decreases slowly after it reaches a maximum value. However, near resonance, n_2 behaves differently. For example, at $\Delta_p = 7$ MHz, n_2 keeps increasing as the coupling power increases, as shown in Fig. 3(b), and is limited only by the available coupling power in our experiment. Notice that n_2 is

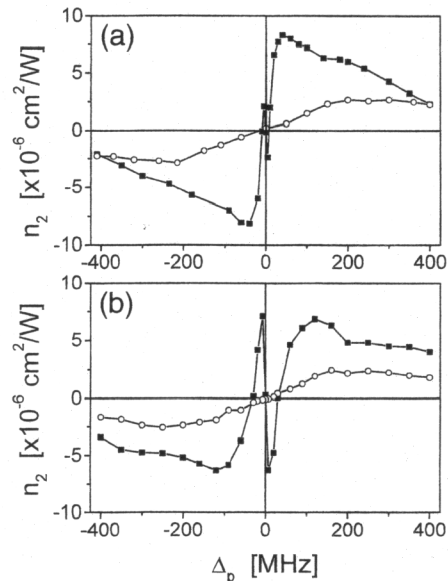


Fig. 2. Measured Kerr-nonlinearity index of refraction n_2 as a function of probe frequency detuning for (a) $\Omega_c = 2\pi \times 17$ MHz and (b) $\Omega_c = 2\pi \times 72$ MHz. $\Omega_p = 2\pi \times 11$ MHz and $\Delta_c = 0$. Filled squares, three-level case; open circles, two-level case ($\Omega_c = 0$).

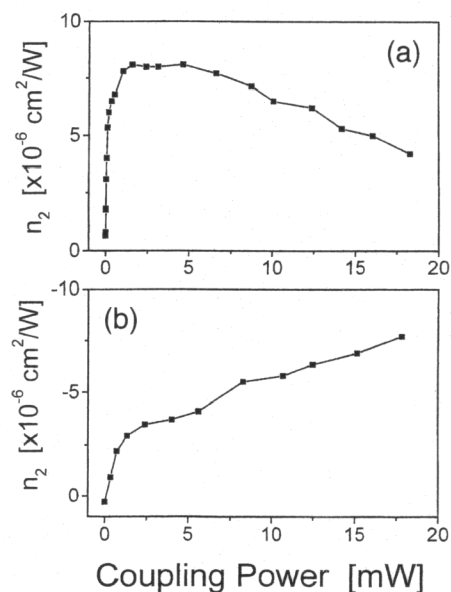


Fig. 3. Measured Kerr-nonlinearity index of refraction n_2 as a function of coupling power for (a) $\Delta_p = 40$ MHz and (b) $\Delta_p = 7$ MHz. $\Omega_p = 2\pi \times 11$ MHz and $\Delta_c = 0$.

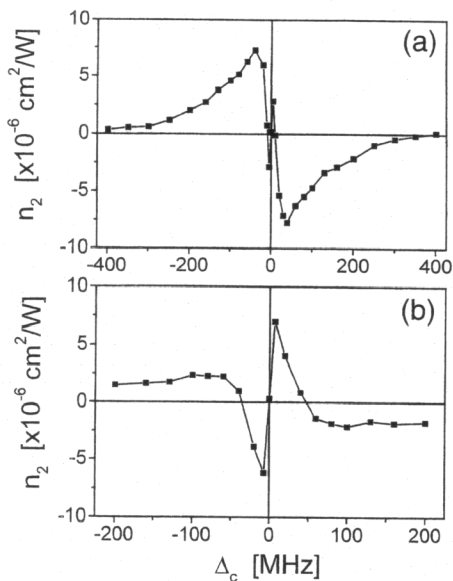


Fig. 4. Measured Kerr-nonlinear index of refraction n_2 as a function of coupling frequency detuning Δ_c for (a) $\Omega_c = 2\pi \times 17$ MHz and (b) $\Omega_c = 2\pi \times 72$ MHz. $\Omega_p = 2\pi \times 11$ MHz and $\Delta_p = 0$.

positive for $\Delta_p = +40$ MHz but becomes negative for $\Delta_p = +7$ MHz.

The enhanced Kerr-nonlinear coefficient is caused by atomic coherence in the three-level atoms. The central peaks are related to the EIT dip and decrease as the absorption reduction decreases (with reduced coupling power). The outer peaks are related to the Rabi sidebands, and, as the coupling power increases, the Rabi sidebands move out owing to power broadening, which also leads to the shift of peaks in n_2 toward larger frequency detunings. We have theoretically treated the case for strong coupling intensity (EIT condition) by using the iteration technique and obtained results that match well the experimentally measured data presented in Fig. 2(b).⁹ However, that technique does not apply to the weak-coupling case, and a general theory is needed to treat the enhancement of Kerr nonlinearity with an arbitrary coupling intensity-to-probe intensity ratio.

We also studied the dependence of n_2 on Δ_c for weak and strong coupling beams. Figures 4(a) and 4(b) plot n_2 as a function of Δ_c for $\Omega_c = 2\pi \times 17$ and $\Omega_c = 2\pi \times 72$ MHz, respectively, with $\Omega_p = 2\pi \times 11$ MHz and $\Delta_p = 0$. For a strong coupling beam [Fig. 4(b)], the increase in n_2 for Δ_c beyond ± 100 MHz is due simply to optical pumping. However, with a weak coupling beam the n_2 enhancement occurs over much larger coupling frequency detuning ranges (as large as ± 200 MHz). Such large changes in n_2 enable us to control nonlinear optical processes in multilevel atomic systems and eventually lead to useful applications.

We point out that the measured n_2 in this study is related to self-phase modulation from $n = n_0 + n_2 I_p$,

i.e., from an index change in the probe beam owing to its own intensity I_p . The Kerr-nonlinearity enhancements reported earlier were related to the cross-phase modulation from $n' = n_0' + n_2' I_c$, i.e., the index change for the probe beam that was due to the intensity of another (coupling) beam.¹² In the latter case, n_2' is directly proportional to the increased linear dispersion slope or to the reduced group velocity.^{12,13} The change in n_2 as a function of I_c , as measured in this study, should be considered as the nonlinear self-phase-modulation effect, which is different from the change in the n_2' term.

In summary, we have experimentally studied the Kerr-nonlinear index of refraction in a three-level Λ -type atomic system for several coupling powers and found that the Kerr nonlinearity is greatly enhanced because of atomic coherence in the three-level atomic system compared with that in a two-level atomic system. The coupling power, coupling frequency detuning, and probe frequency detuning can all dramatically alter the Kerr-nonlinear coefficient in such a three-level atomic system. Kerr nonlinearity can be enhanced to the same level for weak coupling power as for much stronger coupling power, which provides us with a road map to achieving large nonlinear optical effects at low light levels.

This research was supported in part by the National Science Foundation. M. Xiao's e-mail address is mxiao@mail.uark.edu.

*Present address, Institute of Opto-Electronics, Shanxi University, Shanxi, China.

References

1. K. Hakuta, L. Marmet, and B. P. Stoicheff, *Phys. Rev. Lett.* **66**, 596 (1991).
2. A. J. Merriam, S. J. Sharpe, M. Shverdin, D. Manuszak, G. Y. Yin, and S. E. Harris, *Phys. Rev. Lett.* **84**, 5308 (2000).
3. P. R. Hemmer, D. P. Katz, J. Donoghue, M. Cronin-Golomb, M. S. Shahriar, and P. Kumar, *Opt. Lett.* **20**, 982 (1995).
4. B. Lu, W. H. Burkett, and M. Xiao, *Opt. Lett.* **23**, 804 (1998).
5. M. Yan, E. G. Rickey, and Y. Zhu, *Opt. Lett.* **26**, 548 (2001).
6. S. E. Harris and L. Hau, *Phys. Rev. Lett.* **82**, 4611 (1999).
7. S. E. Harris and Y. Yamamoto, *Phys. Rev. Lett.* **81**, 3611 (1998).
8. A. Imamoglu, H. Schmidt, G. Woods, and M. Deutsch, *Phys. Rev. Lett.* **79**, 1467 (1997).
9. H. Wang, D. J. Goorskey, and M. Xiao, *Phys. Rev. Lett.* **87**, 073601-1 (2001).
10. J. Gea-Banacloche, Y. Li, S. Jin, and M. Xiao, *Phys. Rev. A* **51**, 576 (1995).
11. Y. Li and M. Xiao, *Phys. Rev. A* **51**, R2703 (1995).
12. L. V. Hau, S. E. Harris, Z. Dutton, and C. H. Behroozi, *Nature* **397**, 594 (1999).
13. M. Xiao, Y. Li, S. Jin, and J. Gea-Banacloche, *Phys. Rev. Lett.* **74**, 666 (1995).